PHYSICAL REVIEW B **88**, 201101(R) (2013)

Unconventional magnetism in multivalent charge-ordered $YbPtGe_2$ probed by ^{195}Pt- and ^{171}Yb-NMR

R. Sarkar,* R. Gumeniuk, A. Leithe-Jasper, W. Schnelle, Y. Grin, C. Geibel, and M. Baenitz
Max Planck Institute for Chemical Physics of Solids, 01187 Dresden, Germany
(Received 6 September 2013; published 1 November 2013)

Detailed ^{195}Pt and ^{171}Yb nuclear magnetic resonance (NMR) studies on the heterogeneous mixed valence system $YbPtGe_2$ are reported. The temperature dependence of the ^{195}Pt-NMR shift $^{195}K(T)$ indicates the opening of an unusual magnetic gap below 200 K. $^{195}K(T)$ was analyzed by a thermal activation model which yields an isotropic gap $\Delta/k_B \approx 200$ K. In contrast, the spin-lattice relaxation rate $^{195}(1/T_1)$ does not provide evidence for the gap. Therefore, an intermediate-valence picture is proposed while a Kondo-insulator scenario can be excluded. Moreover, $^{195}(1/T_1)$ follows a simple metallic behavior, similar to the reference compound $YPtGe_2$. A well-resolved NMR line with small shift is assigned to divalent ^{171}Yb. This finding supports the proposed model with two subsets of Yb species (di- and trivalent) located on the Yb2 and Yb1 site of the $YbPtGe_2$ lattice.

DOI: 10.1103/PhysRevB.88.201101 PACS number(s): 75.30.Mb, 76.60.−k, 75.20.Hr

Intermetallic compounds formed by d-transition metals with mostly itinerant electrons and rare-earth metals with more localized electrons ($4f$ electrons) have been the subject of intense research activities in solid state science. The importance of these systems is the presence of an effective hybridization between localized and itinerant electrons giving rise to exotic properties such as mixed- or intermediate-valence states, heavy-fermion and non-Fermi-liquid behaviors, unconventional superconductivity, Kondo insulators, Kondo semiconductors, and quantum criticality.[1–4]

Among the properties listed above the heavy-fermion semiconductors, alternately called Kondo insulators, have attracted much attention in recent years. These materials exhibit a small energy gap at the Fermi level, which is believed to appear due to the hybridization between localized d or f electrons with conduction electrons. Kondo insulators associated with such a hybridization gap are characterized by an insulating or semiconducting electrical resistivity, a nonmagnetic ground state, and local-moment magnetism at temperatures far above the gap opening. The best known examples of such materials are YbB_{12},[5–7] $Ce_3Bi_4Pt_3$,[8,9] FeSi,[2,10] U_2Ru_2Sn,[11] $CeRu_4Sn_6$,[12] and $CeFe_2Al_{10}$.[13] There are also Kondo insulators which exhibit metal-like electrical resistivity at low temperatures, caused by residual "in-gap states" and an anisotropic Fermi surface. Typical examples are CeNiSn,[14] $CeRu_4Sn_6$,[12] and SmB_6.[15] Just recently these "in-gap states" received revived attention because the question arises as to whether such states are actually metallic surfaces of a three-dimensional topological insulator.[16,17]

In this context the very recently studied intermetallic compound $YbPtGe_2$ deserves particular interest. $YbPtGe_2$ crystallizes with the $YIrGe_2$ type (space group $Immm$, $a = 4.33715$ Å, $b = 8.73518$ Å, and $c = 16.14684$ Å.[18] As shown in Fig. 1, two Yb atoms occupy the $4i$ (Yb1) and $4g$ (Yb2) sites, three Ge atoms are located at $4j$ (Ge1), $8m$ (Ge2), and $8l$ (Ge3) sites, and one Pt atom at the $8l$ site in the unit cell. The different bonding situation suggests dissimilar valence states between Yb1 and Yb2 sites. The species on the Yb1 site, which has a coordination polyhedron of rather small volume, may be considered as an electronic configuration close to $4f^{13}$ (magnetic trivalent Yb). On the other hand, the atoms on the Yb2 site within a quite large hexagonal prismatic coordination polyhedron are expected to have the $4f^{14}$ configuration (nonmagnetic divalent Yb).[18]

Because of two inequivalent crystallographic sites of Yb with different electronic configurations, $YbPtGe_2$ is considered as a multivalent charge-ordered system. Moreover, a huge drop of the magnetic susceptibility (χ) in the temperature range of 50–200 K could not be explained by the simple valence fluctuations model.[18] Such a drop in χ is reminiscent of correlated semiconductors and/or semimetals such as YbB_{12},[5] $Ce_3Bi_4Pt_3$,[19] FeSi,[2] U_2Ru_2Sn,[11] and $CeFe_2Al_{10}$.[13] However, unlike the other Kondo semiconductors, we have not found any clear sign of a charge gap in the electrical resistivity of $YbPtGe_2$.[18] Therefore the present system has been assigned as a compound with an unconventional pseudogap.

Nuclear magnetic resonance (NMR) is a local probe, and therefore the NMR shift $K \sim \chi$ provides information about the local uniform susceptibility $\chi(q = 0,\omega = 0)$. The spin-lattice relaxation rate $[1/T_1 \sim \sum_q A_q \chi'(q,\omega)]$ supplies information about the dynamic susceptibility $\chi'(q,w)$ and the hyperfine form factor A_q. In the framework of the Korringa relation, $1/T_1$ gives a direct estimate for the density of states (DOS) at the Fermi level if the exchange enhancement in the metal is not too large.

Therefore NMR has been extensively and successfully applied to understand the microscopic magnetic properties of correlated semimetal and/or pseudogapped systems. While we have reported the ^{195}Pt NMR shift data incorporated with the bulk susceptibility data briefly,[18] we present here a more detailed and extended NMR study on $YbPtGe_2$.

$YbPtGe_2$ powder samples were prepared according to Ref. 18. The powder was mixed with paraffin in a small quartz tube, subsequently heated up and shaken up, and then cured to randomize the grains. Because of the high NMR frequency and the metallic nature of the material such process is required to prevent the reduction of the NMR signal due to a finite skin depth associated with radio-frequency penetration for resonance. The first field sweep NMR measurements were carried out using a conventional pulsed NMR technique on ^{195}Pt nuclei (nuclear spin $I = 1/2$ and $\gamma = 9.09$ MHz/T)[20] in the temperature range of 4.2 K $\leqslant T \leqslant$ 295 K at fixed

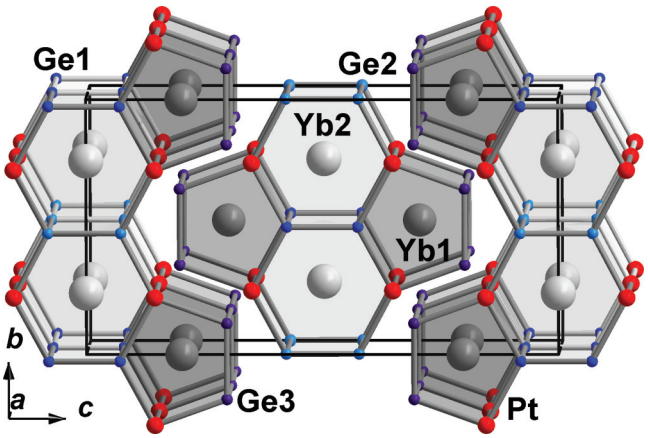

FIG. 1. (Color online) Crystal structure of $YbPtGe_2$.

frequencies of 45 and 24 MHz. The ^{195}Pt NMR shift has been determined with respect to the nonmagnetic reference compound $YPtGe_2$[21] with $^{195}K \approx 0$. Therefore the $K(T)$ values are regarded as the pure $4f$ shift component K_{4f} where a small residual temperature-independent K_0 component is already corrected. K_0 is the conduction electron contribution from the trivalent reference. The field sweep spectra are obtained by integration over the spin echo in the time domain at a given field. The powder spectra are fitted with an anisotropic shift tensor to determine the components for the a, b, and c directions. The isotropic part of the Knight shift, $^{195}K_{\rm iso}$, has been determined by $^{195}K_{\rm iso} = (K_a + K_b + K_c)/3$. The spin-lattice relaxation rate $^{195}(1/T_1)$ has been measured by the standard saturation recovery method in different external magnetic fields. Additionally, we succeeded in observing the ^{171}Yb NMR, and the discussion of the characteristic features of the spectra is also described below.

Figure 2 shows the ^{195}Pt field sweep NMR spectra at different temperatures at a fixed frequency of 45 MHz. In all temperatures a typical powder spectrum with three singularities at K_α (α being a, b, and c) are observed. The spectra can be analyzed convincingly with the consideration of typical random powder pattern for a spin $I = 1/2$ nuclei with an anisotropic shift tensor caused by the orthorhombic point symmetry. We have analyzed the spectra with three different shift values K_a, K_b, and K_c. The lines in Fig. 2 indicate the best fits. With lowering the temperature the whole spectra are shifted initially towards the high-field side and then move towards the low-field side. However, in the temperature range 30–1.8 K the spectra remain unperturbed with respect to their α coordinate.

One point of interest in Fig. 2 is the absence of drastic changes of the line profile with lowering of the temperature. This suggests that $YbPtGe_2$ does not have any short-range ordering or defects leading to a distribution of internal fields and corresponding NMR line broadening. The estimated ^{195}Pt NMR shift results of $YbPtGe_2$ for the three crystallographic axes together with the isotropic shift are shown in Fig. 3. The temperature dependence of the shifts in the three directions is quite similar, except at high temperatures where K_c is less temperature dependent than K_a and K_b. The remarkably different hyperfine field in the c direction could be related to the slight lattice distortion of this system which affects the

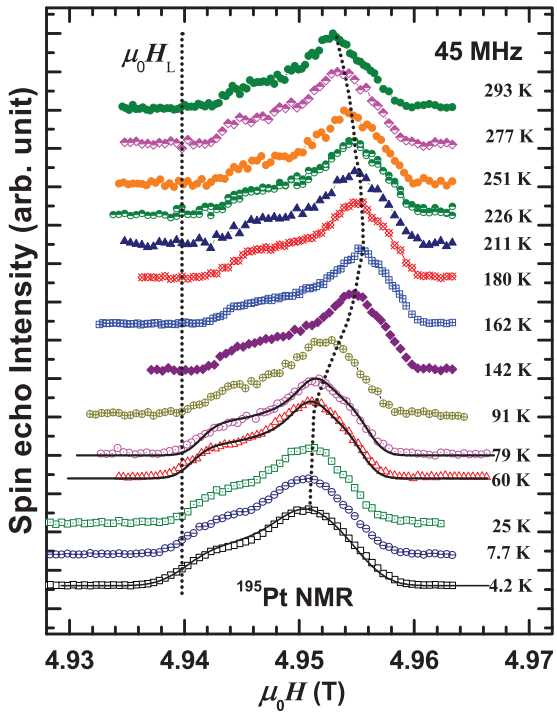

FIG. 2. (Color online) ^{195}Pt field sweep NMR spectra taken at 45 MHz. The solid lines represent theoretical simulations. The dotted curved line is a guide to the eye for the development of the main shift component of the shift tensor. The vertical dotted line indicates the Larmor field for ^{195}Pt from the nonmagnetic reference $YPtGe_2$.

hyperfine field. The isotropic shift $^{195}K_{\rm iso}$ nicely follows the bulk susceptibility,[18] except for $T < 30$ K where a small amount of paramagnetic impurities prevails in the bulk susceptibility ("Curie tail") whereas the shift becomes constant for $T \to 0$. We have already shown the shift to be proportional to the susceptibility with the temperature as an implicit parameter

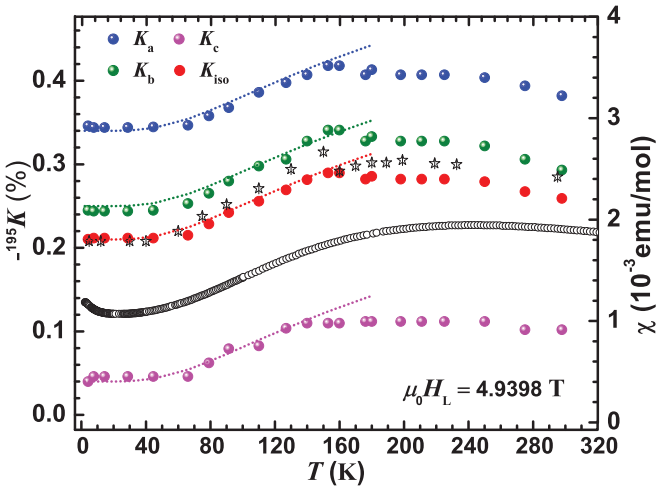

FIG. 3. (Color online) Temperature dependence of the ^{195}Pt NMR shift components $^{195}K_\alpha$ ($\alpha = a, b, c$) and the isotropic shift $^{195}K_{\rm iso}$ in $YPtGe_2$ as estimated from the theoretical fits. $^{195}K_{\rm iso}$ for 45 MHz (•, red) and 24 MHz (⋆, black); see text. Also the bulk magnetic susceptibility (Ref. 18) is shown (○, black). The dotted line represents the activation gap model.

by a K-χ plot ("Clogston-Jaccarino" plot).[22] The observed isotropic shift is related to the magnetic bulk susceptibility by the expression

$$K_{\rm iso}(T) = K_0 + A_{\rm hf}\chi(T)/N_A\mu_B, \quad (1)$$

where $A_{\rm hf}$ is the hyperfine coupling constant, χ is the bulk magnetic susceptibility, and K_0 is a residual temperature-independent shift contribution. We obtain the hyperfine coupling constant of $A_{\rm hf} = -7.261$ kOe/μ_B and $K_0 = -0.21\%$. In the K-χ plot at high temperatures a change of slope is observed, indicating the change of the hyperfine coupling constant. Finally it should be mentioned that the shift is negative as expected for Yb-based compounds by employing a simple conduction electron polarization model.[23] The finite K_0 value with respect to the nonmagnetic homologue $YPtGe_2$ is due to a conduction electron contribution (positive) and/or a chemical shift contribution (negative).

Following the bulk magnetic susceptibility, the negative shift increases rather sharply with increasing temperature in the range from 35 K to 160 K. Subsequently, the shift exhibits a broad maximum and thereafter decreases slowly following a Curie-Weiss law. The present results are reminiscent of correlated semimetal systems such as YbB_{12},[7] U_2Ru_2Sn,[11] $Ce_3Bi_4Pt_3$,[19] $CeFe_2Al_{10}$,[13] and $U_3Bi_4Ni_3$.[24] The sharp decrease of the shift with a residual shift value of around -0.21% may be interpreted as the opening of a pseudogap at the Fermi energy. To get an idea of the gap size of this system, we have fitted the $^{195}K^{\alpha}$ data with a simple activation gap model $K_0^{\alpha} + A^{\alpha} \times \exp(-\Delta^{\alpha}/k_BT)$. The fits result in similar gap values for all three direction with gap sizes of $\Delta^{\alpha}/k_B \approx 200$ K. It should be mentioned that the residual shift values K_0^{α} are rather different, which indicates the anisotropy of the electronic band structure of the orthorhombic system.

As already mentioned, $1/T_1$ is very sensitive to the DOS at the Fermi energy. For a simple metal, the following relation is obtained,[25–27]

$$1/T_1 \propto T\sum_q A_q\chi'(q,\omega) \propto \mathcal{K}^2(\alpha)K^2T, \quad (2)$$

where $\mathcal{K}(\alpha)$ is an enhancement factor which depends on $\alpha \propto \chi'(q \neq 0)/\chi\prime(q = 0)$ according to the Stoner theory.[25–27] If the enhancement factor $\mathcal{K}(\alpha) = 1$, then Eq. (2) becomes

$$1/T_1TK^2 = S_0, \quad (3)$$

which is known as the Korringa relation and S_0 is the Korringa product. To see the effect of this pseudogap on the dynamical susceptibility $\chi'(q,\omega)$, we have also investigated the spin-lattice relaxation rate $^{195}(1/T_1)$, which is a direct measure of the DOS. With the opening of a gap, $^{195}(1/T_1)$ should decrease drastically and, in a simple activation gap model, it should decrease exponentially; i.e., $^{195}(1/T_1) \propto \exp(-\Delta/k_BT)$. For spin $I = 1/2$ nuclei the magnetization recovery curve should be followed by the equation

$$1 - M(t)/M(0) = A\exp(-t/T_1), \quad (4)$$

where $M(t)$ is the magnetization at a time t after the saturation pulse and $M(0)$ is the equilibrium magnetization.

In our experiments all magnetization recovery curves follow Eq. (4) and by fitting $^{195}(1/T_1)$ was estimated. Figure 4 shows the $^{195}(1/T_1)$ vs T plot at two different fields for

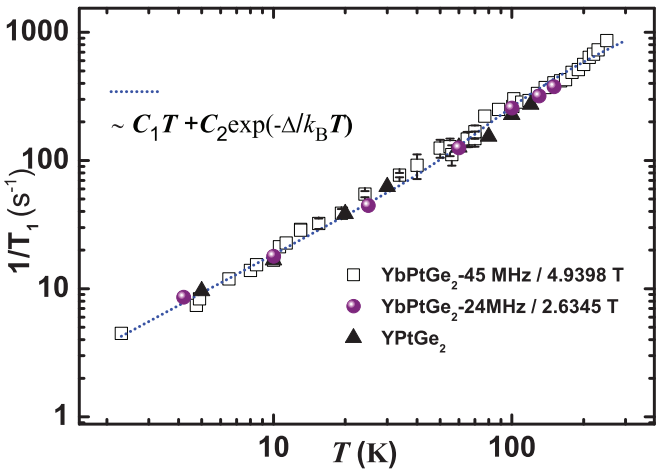

FIG. 4. (Color online) ^{195}Pt spin-lattice relaxation rate vs T plot at frequencies 24 and 45 MHz for $YbPtGe_2$. In addition, $^{195}(1/T_1)$ of the nonmagnetic reference compound $YPtGe_2$ is plotted. The dashed line represents a pseudogap fit (see text).

$YbPtGe_2$ and the reference compound $YPtGe_2$. One can immediately recognize that the temperature dependence of $^{195}(1/T_1)$ in $YbPtGe_2$ is nearly identical to that of nonmagnetic $YPtGe_2$. The dashed line is a fit with a pseudogap model[11] where only a small fraction of states are gapped and the rest remain nongapped. Such a scenario implies a large number of nongapped states which is less realistic. Another reason might be that the magnetic fluctuations are filtered out by the hyperfine form factor A_q at the Pt site.

In most Kondo insulators, the opening of the gap is evidenced by a considerable drop in the $1/T_1$ vs T plot, such as in U_2Ru_2Sn and FeSi. This further indicates that the Yb $4f$-electron dynamical spin and/or charge fluctuations do not at all influence the ^{195}Pt nuclei, and, seemingly $^{195}(1/T_1)$ is insensitive to the spin and/or charge excitations. Most probably the uniform susceptibility deviates strongly from the complex q-dependent dynamic susceptibility $\chi'(q,\omega)$. It is worth mentioning here that there exists no clear evidence of the gap in electrical resistivity data, which behave like a simple metal as in the $^{195}(1/T_1)$ results. Therefore, from the $^{195}(1/T_1)$ data we rule out a Kondo-insulator scenario for $YbPtGe_2$.

The aforementioned model with two different Yb species (nearly divalent Yb on the Yb2 site, nearly trivalent magnetic Yb on the Yb1 site) opens up the opportunity to probe the nonmagnetic Yb ion on the Yb2 site by NMR, which is a rare case (^{171}Yb, $I = 1/2$, $\gamma = 7.4987$ MHz/T). We focused our NMR study on selected frequencies (fields) as indicated in Fig. 5. The ^{171}Yb NMR line was obtained at several frequencies. In Fig. 5(b) the evolution of the resonance frequency of the center line (illustrated with a spectra) with the resonance field at 4.2 K is shown. The slope of the line roughly corresponds to the textbook γ value for ^{171}Yb (average value 7.4575 MHz/T). The shape of the field sweep NMR spectra clearly reveals the orthorhombic site symmetry [Figs. 5(a) and 5(c)]. The line position itself is very close to the Larmor field of ^{171}Yb which further corroborates that we are probing the nonmagnetic ions on the Yb2 site of the $YbPtGe_2$ lattice [cf. Fig. 5(b)]. In contrast to Pt, the Yb2 site seems to be weakly coupled to the magnetic Yb1 site and therefore no

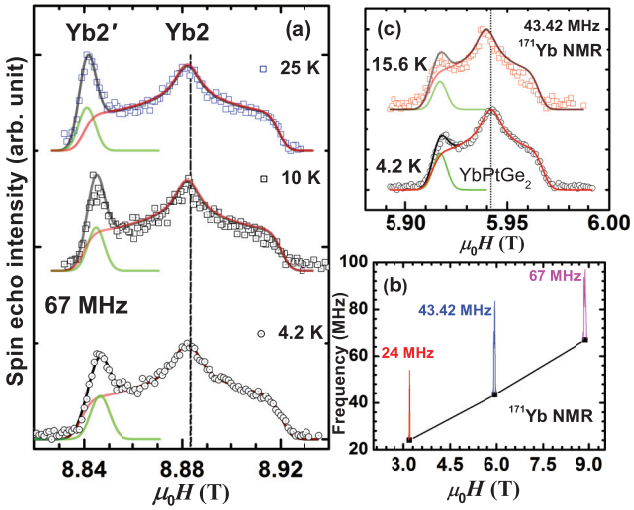

FIG. 5. (Color online) ^{171}Yb field sweep NMR spectra at different frequencies for $YbPtGe_2$. (a) and (c) show the ^{171}Yb spectra at 67 MHz and 43.42 MHz together with the calculation by a model with two Yb2 sites with different anisotropy, respectively. (b) ^{171}Yb field sweep NMR spectra and frequencies as a function of resonance field at 4.2 K. The solid line provides an average γ for Yb.

sizable temperature dependence of the shift is found. The line is consistently (67 MHz and 43.42 MHz) simulated by taking three temperature-independent weak shift tensor components $K_\alpha = +0.5\%$ (left), 0.01% (middle), and -0.48% (right).

Surprisingly, we observe an additional ^{171}Yb NMR line superimposed on the main Yb2 line. This Yb2′ line has also only a weak and temperature-independent shift $K' \cong 0.5\%$ which directly implies that its origin is nonmagnetic Yb^{2+}. Most likely this additional Yb2′ signal is not a foreign phase because it is centered on the left singularity of the main spectrum. We believe that the origin of this line is a partial texture in the powder sample which amplifies the signal in this particular orientation. Such an effect is common in NMR on powder samples.[23]

To sum up, our present Pt-NMR shift investigations tracks down microscopically the bulk susceptibility, evidencing the exotic nature of $YbPtGe_2$. We found an isotropic gap from the shift analysis with $\Delta/k_B \approx 200$ K. The $^{195}(1/T_1)$ results are in good agreement with resistivity data, which shows that there is no charge gap, clearly ruling out a Kondo-insulator scenario.

Further, the dynamical spin fluctuations of the Yb $4f$ electrons seem to be filtered out at the Pt sites, so that $^{195}(1/T_1)$ behaves like a simple metal similar to $YPtGe_2$. It could be speculated that this is due to a complex q dependence of $\chi(q,\omega)$. However, neither the relation $^{195}(1/T_1TK^2) =$ constant (simple metallic) nor $^{195}(1/T_1TK) =$ constant (weakly magnetic) are valid in this system. In good agreement with the suggested scenario[18] of two different Yb species (nearly divalent Yb on Yb2 site, nearly trivalent magnetic Yb on Yb1 site), the NMR gives good evidence for nonmagnetic Yb species on the Yb2 site.

So far, in our NMR investigations, the magnetic Yb^{3+} ion on the Yb1 site could not be found. Magnetic Yb is observed only in the rare cases of some valence-fluctuating systems such as $YbAl_2$ and $YbAl_3$,[28] or YbB_{12}.[29] Here, the residual NMR shift due to the intermediate valence of Yb is very large and not easy to detect.[28,29] The on-site interaction in these Yb systems is well understood and allows the calculation of the shift from the Yb-dominated bulk susceptibility.[30] Our NMR data clearly reveal the presence of well-ordered Yb^{2+} species with orthorhombic site symmetry. This finding is a microscopic proof for the proposed multivalent charge-ordered system scenario.

We acknowledge Prof. Hiroshi Yasuoka for stimulating discussions. R. Sarkar is grateful to the DFG for financial support through Grant No. SA 2426/1-1.

*Present address: Institute for Solid State Physics, TU Dresden, 01069 Dresden, Germany; rajibsarkarsinp@gmail.com

[1] D. Adroja, K. Mcewen, J.-G. Park, A. Hillier, N. Takeda, P. Riseborough, and T. Takabatake, J. Optoelectronics Advanced Mat. **10**, 1719 (2008).

[2] P. Riseborough, Adv. Phys. **49**, 257 (2000).

[3] G. R. Stewart, Rev. Mod. Phys. **73**, 797 (2001).

[4] A. Georges, G. Kotliar, W. Krauth, and M. J. Rozenberg, Rev. Mod. Phys. **68**, 13 (1996).

[5] M. Kasaya, F. Iga, K. Negishi, S. Nakai, and T. Kasuya, J. Magn. Magn. Mater. **31–34**, 437 (1983).

[6] F. Iga, M. Kasaya, and T. Kasuya, J. Magn. Magn. Mater. **76–77**, 156 (1988).

[7] M. Kasaya, F. Iga, M. Takigawa, and T. Kasuya, J. Magn. Magn. Mater. **47–48**, 429 (1985).

[8] M. F. Hundley, P. C. Canfield, J. D. Thompson, Z. Fisk, and J. M. Lawrence, Phys. Rev. B **42**, 6842 (1990).

[9] M. Jaime, R. Movshovich, G. R. Stewart, W. P. Beyermann, M. G. Berisso, M. F. Hundley, P. C. Canfield, and J. L. Sarrao, Nature (London) **405**, 160 (2000).

[10] V. Jaccarino, G. K. Wertheim, J. H. Wernick, L. R. Walker, and S. Arajs, Phys. Rev. **160**, 476 (1967).

[11] A. K. Rajarajan, A. Rabis, M. Baenitz, A. A. Gippius, E. N. Morozowa, J. A. Mydosh, and F. Steglich, Phys. Rev. B **76**, 024424 (2007).

[12] E. M. Brüning, M. Brando, M. Baenitz, A. Bentien, A. M. Strydom, R. E. Walstedt, and F. Steglich, Phys. Rev. B **82**, 125115 (2010).

[13] S. C. Chen and C. S. Lue, Phys. Rev. B **81**, 075113 (2010).

[14] T. Takabatake, F. Teshima, H. Fujii, S. Nishigori, T. Suzuki, T. Fujita, Y. Yamaguchi, J. Sakurai, and D. Jaccard, Phys. Rev. B **41**, 9607 (1990).

[15] J. C. Cooley, M. C. Aronson, Z. Fisk, and P. C. Canfield, Phys. Rev. Lett. **74**, 1629 (1995).

[16] M. Dzero, K. Sun, V. Galitski, and P. Coleman, Phys. Rev. Lett. **104**, 106408 (2010).

[17] M. Dzero, K. Sun, P. Coleman, and V. Galitski, Phys. Rev. B **85**, 045130 (2012).

[18] R. Gumeniuk, R. Sarkar, C. Geibel, W. Schnelle, C. Paulmann, M. Baenitz, A. A. Tsirlin, V. Guritanu, J. Sichelschmidt, Y. Grin, and A. Leithe-Jasper, Phys. Rev. B **86**, 235138 (2012).

[19] A. P. Reyes, R. H. Heffner, P. C. Canfield, J. D. Thompson, and Z. Fisk, Phys. Rev. B **49**, 16321 (1994).

[20] M. Baenitz, R. Sarkar, R. Gumeniuk, A. Leithe-Jasper, W. Schnelle, H. Rosner, U. Burkhardt, M. Schmidt, U. Schwarz, D. Kaczorowski, Y. Grin, and F. Steglich, Phys. Status Solidi B **247**, 740 (2010).

[21] M. François, G. Venturini, E. McRae, B. Malaman, and B. Roques, J. Less Common Metals **128**, 249 (1987).

[22] A. M. Clogston, V. Jaccarino, and Y. Yafet, Phys. Rev. **134**, A650 (1964).

[23] G. C. Carter, L. H. Bennett, and D. J. Kahan, *Metallic Shifts in NMR*, Progress in Materials Science (Pergamon Press, New York, 1977).

[24] S.-H. Baek, N. J. Curro, T. Klimczuk, H. Sakai, E. D. Bauer, F. Ronning, and J. D. Thompson, Phys. Rev. B **79**, 195120 (2009).

[25] H. Tou, K. Ishida, and Y. Kitaoka, J. Phys. Soc. Jpn. **74**, 1245 (2005).

[26] M. Baenitz, R. Sarkar, P. Khuntia, C. Krellner, C. Geibel, and F. Steglich, Phys. Status Solidi C **10**, 540 (2013).

[27] R. Sarkar, P. Khuntia, J. Spehling, C. Krellner, C. Geibel, H.-H. Klauss, and M. Baenitz, Phys. Status Solidi B **250**, 519 (2013).

[28] T. Shimizu, M. Takigawa, H. Yasuoka, and J. H. Wernick, J. Magn. Magn. Mater. **52**, 187 (1985).

[29] K. Ikushima, Y. Kato, M. Takigawa, F. Iga, S. Hiura, and T. Takabatake, Physica B: Condensed Matter **281–282**, 274 (2000).

[30] Assuming a hyperfine form factor $A_{\mathrm{Yb}}^{\mathrm{hf}} = 115\,\mathrm{T}/\mu_B$ leads to a shift of ≈67% for the $^{171}Yb^{3+}$ line in $YbPtGe_2$: $H_{\mathrm{res}}^{\mathrm{Yb}} = H_L/(1 + \chi A_{\mathrm{hf}}^{\mathrm{Yb}}) \approx H_L/(1 + 0.495) \approx 0.67 H_L$, where H_L is the Larmor field of ^{171}Yb and χ the susceptibility in units of $[\mu_B/\mathrm{T}]$.